



1 **Glacier melting and precipitation trends detected by surface area 2 changes in Himalayan ponds**

3 Franco Salerno^(1,3), Sudeep Thakuri^(1,3), Nicolas Guyennon⁽²⁾, Gaetano Viviano⁽¹⁾, Gianni Tartari^(1,3)

4 ⁽¹⁾ National Research Council, Water Research Institute, Brugherio (IRSA -CNR), Italy

5 ⁽²⁾ National Research Council, Water Research Institute, Roma (IRSA-CNR), Italy

6 ⁽³⁾ Ev-K2-CNR Committee, Via San Bernardino, 145, Bergamo 24126, Italy

7 *Correspondence to Franco Salerno (salerno@irsa.cnr.it)*

8 **Abstract.** Climatic time series for high-elevation Himalayan regions are decidedly scarce. Although
9 glacier shrinkage is now sufficiently well described, the changes in precipitation and temperature at these
10 elevations are less clear. This contribution shows that the surface area variations of unconnected glacial
11 ponds, i.e., ponds not directly connected to glaciers, can be considered suitable proxies for detecting
12 changes in the main hydrological components of the water balance on the south side of Mt. Everest.
13 Glacier melt and precipitation trends have been inferred by analyzing the surface area variations of ponds
14 with various degrees of glacial coverage within the basin. In general, unconnected ponds over the last
15 fifty years (1963-2013 period) have decreased significantly by approximately 10%. We inferred an
16 increase in precipitation occurred until the mid-1990s followed by a decrease until recent years. Until the
17 1990s, glacier melt was constant. An increase occurred in the early 2000s, and in the recent years,
18 contrasting the observed glacier reduction, a declining trend in maximum temperature has decreased the
19 glacier melt.

20 **1 Introduction**

21 Meteorological measurements in high-elevation Himalayan regions are scarce due to the harsh
22 conditions of these environments, which limit the suitable maintenance of weather stations (e.g., Vuille,
23 2011; Salerno et al., 2015). Consequently, the availability of long series is even more rare (Barry, 2012;
24 Rangwala and Miller, 2012; Pepin et al., 2015). Generally, gridded and reanalysis meteorological data are
25 used to overcome this lack of data and can be considered an alternative (e.g., Yao et al., 2012). However,
26 in these remote environments their use for climate change impact studies at the synoptic scale must be
27 performed with caution due to the absence of weather stations across the overall region, which limits the
28 ability to perform land-based evaluations of these products (e.g., Xie et al., 2007). Consequently, the
29 meager knowledge on how the climate has changed in recent decades in high-elevation Himalayan
30 regions presents a serious challenge to interpreting the relationships between causes and recently
31 observed effects on the cryosphere. Although glaciers reduction in the Himalaya is now sufficiently well
32 described (Bolch et al., 2012; Yao et al., 2012, Kääb, et al., 2012), the manner in which changes in climate
33 drivers (precipitation and temperature) have influenced the shrinkage and melting processes is less clear
34 (e.g., Bolch et al., 2012; Salerno et al., 2015), and this lack of understanding is amplified when forecasts
35 are conducted.

36 In this context, a substantial body of research has already demonstrated the high sensitivity of lakes
37 and ponds to climate (e.g., Pham et al., 2008; Williamson et al., 2008; Adrian et al., 2009; Lami et al.,
38 2010). Some climate-related signals are highly visible and easily measurable in lakes. For example,



39 climate-driven fluctuations in lake surface areas have been observed in many remote sites. Smol and
40 Douglas (2007) reported decadal-scale drying of high Arctic ponds due to changes in the ratio of
41 precipitation to evaporation. Smith et al. (2005), among other authors, found that lakes in areas of
42 discontinuous permafrost in Alaska and Siberia have disappeared in recent decades. In the Italian Alps,
43 Salerno et al. (2014a) found that since the 1980s, lower-elevation ponds have experienced surface area
44 reductions due to increased evaporation/precipitation ratio, while higher-elevation ponds have increased
45 in size and new ponds have appeared as a consequence of glacial retreat.

46 In high Asian mountains and in particular in the interior of the Tibetan Plateau, the observed lake
47 growth since the late 1990s is mainly attributed to increased precipitation and decreased evaporation (Lei
48 et al., 2014; Song et al., 2015). In contrast, Zhang et al., 2015, attribute the observed increases in lake
49 surface areas since the 1990s across entire Pamir-Hindu Kush-Karakoram-Himalaya region and the
50 Tibetan Plateau region to enhanced glacier melting. Wang et al., 2015, reached similar conclusions in a
51 basin located in the south-central Himalaya. In our opinion, the divergences in the causes leading to the
52 lake surface area variations in central Asia are due to the types of glacial lakes considered in these studies,
53 which could be differentiated in relation to some features of glaciers located within their basin.

54 In general, in high Asian mountains, three types of glacial lakes can be distinguished according to
55 Ageta et al. (2000) and Salerno et al. (2012): (i) lakes that are not directly connected with glaciers but that
56 may have a glacier located in their basin (unconnected glacial lakes); (ii) supraglacial lakes, which
57 develop on the surface of a downstream portion of a glacier; and (iii) proglacial lakes, which are moraine-
58 dammed lakes that are in contact with the glacier front. Some of these lakes store large quantities of water
59 and are susceptible to glacial lake outburst floods (GLOFs). Therefore, in the Himalaya, the potential risk
60 of GLOFs has been, with good reason, widely investigated (e.g., Richardson and Reynolds, 2000; Benn et
61 al., 2012). Factors controlling the growth of these lakes depend on the glacier features from which they
62 develop (surface gradient, mass balance, cumulative surface lowering, and surface velocity) (Reynolds,
63 2000; Quincey et al., 2007; Sakai and Fujita, 2010; Salerno et al., 2012; Sakai, 2012, Thakuri et al.,
64 2015). The causes of proglacial lake development are decidedly similar, and supraglacial lakes are
65 potential precursors of these lakes (e.g., Bolch et al., 2008; Salerno et al., 2012; Thakuri et al., 2015).
66 Their filling and drainage is linked to the supply of meltwater from snow or glacial sources (Benn et al.,
67 2001; Liu et al., 2015), and the opening and closure of englacial conduits (Gulley and Benn, 2007).
68 Therefore, whereas the lake surface area variations of supraglacial and proglacial lakes are strictly related
69 to glacier dynamics, the variations in unconnected glacial lakes are only influenced by glacier melting and
70 precipitation. The different water sources make unconnected glacial lakes potential indicators of changes
71 in the overall water balance components in high-elevation lake basins, such as precipitation, glacier
72 melting, and evapotranspiration.

73 An valuable opportunity for a fine-scale investigation on climate-driven fluctuations in lake surface
74 area is particularly evident on the south slopes of Mt. Everest (Nepal), which is one of the most heavily
75 glaciated parts of the Himalaya (Scherler et al., 2011). Additionally, this region is also characterized by
76 the most glacial lakes in the overall Hindu-Kush-Himalaya range (Gardelle et al., 2011), and a twenty-
77 year series of temperature and precipitation data has recently been reconstructed for these high elevations
78 (5000 m a.s.l.) (Salerno et al., 2015). Moreover, the reduced dimensions of the water bodies in this region,
79 which we can define as ponds according to Hamerlik et al. (2013) (a threshold of $2 \cdot 10^4 \text{ m}^2$ exists between
80 ponds and lakes), make these environments especially susceptible to the effects of climatic changes
81 because of their relatively low water volumes and high surface area to depth ratios (Buraschi et al., 2005;
82 Beniston, 2006).

83 This contribution examines the surface area changes of unconnected glacial ponds on the south side of



84 Mt. Everest (an example is shown in Figure 1) during the last fifty years to evaluate whether they act as
85 potential indicators of changes in the main components of the hydrological cycle (precipitation, glacier
86 melting, and evapotranspiration) at high elevations in the Himalayan range.

87 **2 Region of investigation.**

88 The current study is focused on the southern Koshi (KO) Basin, which is located in the eastern part of
89 central Himalaya (CH) (Yao et al., 2012; Thakuri et al., 2014) (Fig. 2). In particular, the region of
90 investigation is the southern slopes of Mt. Everest in Sagarmatha (Mt. Everest) National Park (SNP)
91 (27.75° to 28.11° N; 85.98° to 86.51° E) (Fig. 2a) (Amatya et al., 2010; Salerno et al., 2010). The SNP
92 (1148 km²) is the highest protected area in the world, extending from an elevation of 2845 to 8848 m a.s.l.
93 (Salerno et al., 2013). Land cover classification shows that almost one-third of the territory is
94 characterized by temperate glaciers and that less than 10% of the park area is forested (Bajracharya et al.,
95 2010), mainly with *Abies spectabilis* and *Betula utilis* (Bhuju et al., 2010).

96 The climate is characterized by monsoons, with a prevailing S-N direction (Ichiyanagi et al., 2007).
97 For the last twenty years at the Pyramid meteorological station (5050 m a.s.l.) (Fig. 2a), the total annual
98 accumulated precipitation is 446 mm, with a mean annual temperature of -2.45 °C. In total, 90% of the
99 precipitation is concentrated during June–September. The probability of snowfall during these months is
100 very low (4%) but reaches 20% at the annual level. Precipitation linearly increases to an elevation of 2500
101 m and exponentially decreases at higher elevations (Salerno et al., 2015).

102 Most of the large glaciers are debris-covered, i.e., the ablation zone is partially covered with
103 supraglacial debris (e.g., Scherler et al., 2011; Bolch et al., 2011; Thakuri et al., 2014). In the SNP, the
104 glacier surfaces are distributed from approximately 4300 m to above 8000 m a.s.l., with more than 75% of
105 the glacier surfaces lying between 5000 m and 6500 m a.s.l. The area-weighted mean elevation of the
106 glaciers is 5720 m a.s.l. in 2011 (Thakuri et al., 2014). These glaciers are identified as summer-
107 accumulation glaciers that are fed mainly by summer precipitation from the South Asian monsoon system
108 (Ageta and Fujita, 1996).

109 Salerno et al. (2012) realized the complete cadaster of all lakes and ponds in the SNP by digitizing
110 ALOS-08 imagery and assigning each body of water a univocal numerical code (LCN, lake cadaster
111 number) according to Tartari et al. (1998). They reported a total of 624 lakes in the park, including 17
112 proglacial lakes, 437 supraglacial lakes, and 170 unconnected lakes. Previous studies revealed that the
113 areas of proglacial lakes increased on the south slopes of Mt. Everest since the early 1960s (Bolch et al.,
114 2008; Tartari et al., 2008; Gardelle et al., 2011, Thakuri et al., 2015). Many studies have indicated that the
115 current moraine-dammed or ice-dammed lakes are the result of coalescence and growth of supraglacial
116 lakes (e.g., Fujita et al., 2009; Watanabe et al., 2009; Thompson et al., 2012, Salerno et al., 2012). Such
117 lakes pose a potential threat due to GLOFs. Imja Tsho (Lake) is one of the proglacial lakes in the Everest
118 region that developed in the early 1960s as small pond and subsequently continuously expanded (Bolch et
119 al., 2008; Somos-Valenzuela et al., 2014, Fujita et al., 2009; Thakuri et al., 2015).

120 **3 Data and Methods**

121 **3.1 Climatic data.**

122 The monthly mean of daily maximum, minimum, and mean temperature and monthly cumulated
123 precipitation time series used in this study have been recently reconstructed for the elevation of the
124 Pyramid Laboratory (5050 m a.s.l.) (Fig. 2) for the 1994–2013 period (Salerno et al., 2015). The potential



125 evapotranspiration for the period (2003-2013) has been calculated by applying the Jensen and Haise
126 model (Jensen and Haise, 1963) using the mean air temperature and solar radiation recorded continuously
127 during this period at Pyramid Laboratory. The Jensen and Haise model is considered to be one of the most
128 suitable evaporation estimation methods for high elevations (e.g., Gardelle et al., 2011; Salerno et al.,
129 2012).

130 To obtain information on climatic trends in the antecedent period (before the 1990s), we used some
131 regional gridded and reanalysis datasets. We selected the closest grid point to the location of the Pyramid
132 Laboratory, and all data were aggregated monthly to allow a comparison at the relevant time scale. With
133 respect to precipitation, we test the monthly correlation between the Pyramid data and the GPCC (Global
134 Precipitation Climatology Centre), APHRODITE (Asian Precipitation-Highly Resolved Observational
135 Data Integration Towards Evaluation of Water Resources), Era-Interim reanalysis of the European Centre
136 for Medium-Range Weather Forecasts (ECMWF), and CRU (Climate Research Unit -Time Series)
137 datasets. For mean air temperature, we considered the Era-Interim, CRU, GHCN (Global Historical
138 Climatology Centre), and NCEP-CFS (National Centers for Environmental Prediction- Climate Forecast
139 System) datasets, whereas for maximum and minimum temperatures, we used the Era-Interim and NCEP-
140 CFS datasets (details on the gridded and reanalysis products are reported in Table SI1).

141 **3.2 Pond digitization.**

142 Pond surface areas were manually identified and digitized using a morphological map from 1963 and
143 more recent satellite imagery from 1992 to 2013. In total, five intermediate periods (details on data
144 sources are provided in Table SI2) were considered according to the availability of satellite imagery. We
145 selected only those ponds present continuously in all these five periods to exclude possible ephemeral
146 environments.

147 From 2000 (2000-2013 period), due to a wider availability of satellite imagery in the region for the
148 last decade, 10 ponds were selected among the pond population considered in the long-term analysis
149 (1963-2013) to continuously track the inter-annual variations in surface area in the recent years. The
150 largest ponds, free from cloud cover, and with diverse glacier coverages (from 1% to 32%) within their
151 basin were favored in the selection (details on data sources used for these lakes are provided in Table
152 SI3).

153 The intra-annual variability in pond surface area has been investigated throughout the year 2001
154 though the availability of 5 cloud-free satellite images from June to December (details on data sources
155 used for these lakes are provided in Table SI4). The first semester of the year was excluded from the
156 analysis because many ponds were frozen until April/May. Even in this case, ponds were selected based
157 on the absence of cloud cover for all images, and the largest lakes with various degrees of glacial
158 coverage were favored. Thus, 4 lakes with these characteristics were selected, and their intra-annual
159 variability is traced in Figure 3. Based on Figure 3, we observe a common significant increase in pond
160 surface area during the summer months, likely due to monsoon precipitation and high glacier melting
161 rates. The acceleration disappears during the fall. The period from October to December is the best period
162 to select the satellite images necessary for the inter-annual analysis of pond surface area. In fact, during
163 these months, the ponds are not yet frozen, the sky is almost free from cloud cover, and, as observed in
164 Figure 3, the inter-annual analysis is not affected by intra-annual seasonality. Consequently all images for
165 the inter-annual analysis have been selected from these months (Table SI1; Table SI2).

166 **3.3 Glacier surface areas and melt.**



167 Glacier surface areas within the pond basins were derived from the Landsat 8 remote imagery
168 (October 10, 2013) taken by the Operational Land Imager (OLI) with a resolution of 15 m. The satellite
169 imagery used to trace the inter-annual variations in glaciers since the early 1960s is reported in Table SI2.
170 Detailed information of digitization methods are described in Thakuri et al., 2014.

171 To simulate the daily melting of the glaciers associated with the 10 selected ponds, we used a simple
172 T-index model (Hock, 2003). This model is able to generate daily melting discharges as a function of
173 daily air temperature above zero, the glacier elevation bands, and a melt factor ($0.0087 \text{ m d}^{-1} \text{ }^{\circ}\text{C}^{-1}$)
174 provided by Kayastha et al. (2008) from a field study (Glacier AX010) located close to the SNP. The daily
175 temperature at the mean elevation of each glacier has been computed according to the lapse rates reported
176 in Salerno et al., 2015.

177 **3.4 Morphometric parameters.**

178 Such parameters related to the ponds basin as the area, slope, aspect, and elevation were calculated
179 thought the Digital Elevation Model (DEM) derived from the ASTER GDEM. The ASTER GDEM tiles
180 for the Mt. Everest region were downloaded from <http://gdem.ersdac.jspacesystems.or.jp>. The vertical and
181 horizontal accuracy of the GDEM are $\sim 20 \text{ m}$ and $\sim 30 \text{ m}$, respectively
182 (www.jspacesystems.or.jp/ersdac/GDEM/E/4.html). We decided to use the ASTER GDEM instead of the
183 Shuttle Radar Topography Mission (SRTM) DEM considering the higher resolution (30 m and 90 m,
184 respectively) and the large data gaps of the SRTM DEM in this study area (Bolch et al., 2011).
185 Furthermore, the ASTER GDEM shows better performance in mountain terrains (Frey et al., 2012).

186 **3.5 Uncertainty of measurements.**

187 All of the imagery and maps were co-registered in the same coordinate system of WGS 1984 UTM
188 Zone 45N. The Landsat scenes were provided in standard terrain-corrected level (Level 1T) with the use
189 of ground control points (GCPs) and necessary elevation data (<https://earthexplorer.usgs.gov>). The
190 ALOS-08 image used here was orthorectified and corrected for atmospheric effects in Salerno et al.
191 (2012).

192 Concerning the accuracy of the measurements, we refer mainly to the work of Tartari et al. (2008),
193 Salerno et al. (2012), and Salerno et al. (2014a) which address in detail the problem of uncertainty in the
194 morphological measurements related to ponds and glaciers obtained from remote sensing imagery, maps
195 and photos. The uncertainty in the measurement of a shape's dimension is dependent both upon the Linear
196 Error (LE) and its perimeter. In particular for ponds (as discussed also by Fujita et al. (2009), and
197 Gardelle et al. (2011) in the calculation of LE), only the Linear Resolution Error (LRE) needs to be
198 considered as the co-registration error does not play a key role. For instance, the ponds considered here
199 are small, and comparisons are made at the entity level and not at the pixel level. The LRE is limited by
200 the resolution of the source data. In the specific study of temporal variations of ponds, Fujita et al. (2009)
201 and Salerno et al. (2012) assumed an error of ± 0.5 pixels.

202 **3.6 Statistical analysis.**

203 The degree of correlation among the data was verified through the Pearson correlation coefficient (r)
204 after testing that the quantile-quantile plot of model residuals follows a normal distribution (not shown
205 here) (e.g., Venables and Ripley, 2002). All tests are implemented in the software R with the significance



206 level at $p < 0.05$. The normality of the data is tested using the Shapiro–Wilk test (Shapiro and Wilk, 1965;
207 Hervé, 2015). The data were also tested for homogeneity of variance with the Levene's test (Fox and
208 Weisberg, 2011). All comparisons conducted in this study are homoscedastic. We used the paired t-test to
209 compare the means of two normally distributed series. If the series were not normal, as a non-parametric
210 ANOVA, we used the Friedman test for paired comparisons and the post-hoc test according to Nemenyi
211 (Pohlert, 2014), while for non-paired comparisons we applied the Kruskal–Wallis test and the post-hoc
212 test according to Nemenyi–Damico–Wolfe–Dunn (Hothorn et al., 2015). The significance of the temporal
213 trends has been tested using the Mann Kendall test ($p < 0.10$) (Mann, 1945; Kendall, 1975; Guyennon et
214 al., 2013).

215 We conducted a Principal Component Analysis (PCA) as described in Wold et al. (1987) between
216 pond surface area variations and climatic variables to obtain information on relationships among the data
217 and to look for reasons that could justify the observed changes in the ponds size (e.g., Settle et al., 2007;
218 Salerno et al., 2014a,b; Viviano et al., 2014).

219 **4 Results and Discussion**

220 **4.1 Climate reconstruction.**

221 To reconstruct the climatic trends before the 1990s, we compared the annual and seasonal
222 precipitation and temperature time series recorded at Pyramid station since 1994 (Salerno et al., 2015)
223 with selected regional gridded and reanalysis datasets (Table SI1). Table 1 shows the coefficient of
224 correlation found for these comparisons. Era Interim ($r = 0.92$, $p < 0.001$) for mean temperature (Fig. 4a)
225 and GPCC ($r = 0.92$, $p < 0.001$) for precipitation (Fig. 4b) provide the best performance at the annual level.
226 All these comparisons are shown in Figure SI1. We observe that precipitation increased significantly until
227 the middle 1990s (+25.6%, $p < 0.05$, 1970–1995 period), then it started to decrease significantly (-23.9%,
228 $p < 0.01$, 1996–2010 period), as observed by the Pyramid station and described by Salerno et al., 2015.
229 The mean temperature shows a continuous increasing trend ($+0.039^{\circ}\text{C yr}^{-1}$, $p < 0.001$, 1979–2013 period)
230 that has accelerated since the early of 1990s.

231 Furthermore, Table 1 shows the low capability of all the products to correctly simulate monsoon
232 temperatures and in particular the daily maximum ones. Figure SI2a reports these correlations at monthly
233 level, while Figure SI2b highlights the misfit between the temperature trends during the monsoon period.

234 **4.2 Pond and glacier surface area variations.**

235 Among the 170 unconnected ponds inventoried in the 2008 satellite imagery (Salerno et al., 2012), we
236 selected, according to the criteria described above, a total of 64 ponds (approximately 1/3) (Fig. 2a). Table
237 2 provides a general summary of their morphological features. We prefer to use the median values to
238 describe these environments because, in general, we observed that these morphological data do not follow
239 a normal distribution. The population consists of ponds larger than approximately 1 hectare ($1.1 \cdot 10^4 \text{ m}^2$),
240 located on very steep slopes (27°), and mainly oriented toward the south-southeast (159°). These ponds
241 are located at a median elevation of 5181 m a.s.l. and within an elevation zone ranging from 4460 to 5484
242 m a.s.l..

243 The observed changes in the surface area of all the considered ponds are listed in Table 3. In general,
244 all unconnected ponds in the last fifty years (1963–2013) decreased by approximately 10%, with a
245 significant difference based on the Friedman test ($p < 0.01$). Figure 4d and Table 3 show that, until the
246 2000s, the ponds had a slight but not significant increasing trend ($+7 \pm 4\%$, $p > 0.05$). Since 2000, they have



247 decreased significantly ($-1.7 \pm 0.6\% \text{ yr}^{-1}$, $p < 0.001$ corresponding to $-22 \pm 18\%$).

248 As for glaciers, Figure 4c reports the glaciers surface differences observed across the SNP
249 (approximately 400 km^2) observed by Thakuri et al., 2014. They reported a decrease of $-13 \pm 3\%$ from
250 1963 to 2011. We updated this series to 2013 and found a further loss of surface area ($-18 \pm 3\%$). For the
251 glaciers located in the basins with the ponds, we traced changes little bit larger. Their overall surface was
252 32.2 km^2 in 1963 and 25.0 km^2 in 2013, with a decrease of $-26 \pm 20\%$ (Fig. 4c; Table 3). According to
253 many authors (e.g., Loibl et al., 2014), as we observe here, the main losses in area over the last decades in
254 the Himalaya have been observed in smaller glaciers.

255 Once we have analyzed how climate and glacier surface areas have changed over the last fifty years,
256 we can now attempt to understand the causes that have led to the variations observed in the pond
257 population. Usually and intuitively, an increase in glacier melt is associated with a decrease in glacier
258 surface area, as observed here. However, if this inbound component was the most significant element of
259 the water balance, the ponds would be increased. However, the ponds have decreased since 2000s; thus,
260 the weaker precipitation observed in recent decades seems to have played a more determining role.
261 Nonetheless, this analysis is extremely broad because it does not consider, for example, a possible
262 different relationship between pond surface area and the degree of glacier coverage in the basin.
263 Therefore, a deeper analysis has been carried out, as shown in the following, to annually trace the surface
264 areas of 10 selected ponds from 2000 to 2013.

265 **4.3 Analysis of potential drivers of change.**

266 Table 4 provides the morphometric characteristics of 10 selected ponds. We observe that the median
267 features of these ponds are comparable with the entire pond population (Table 2), highlighting the good
268 representativeness of the selected case studies. Figure SI3 shows, for each pond, the annual surface area
269 variations that occurred during the 2000–2013 period. All the selected ponds show a significant ($p < 0.05$)
270 decreasing trend according to what has been observed for the whole pond population during the same
271 period (Table 3; Fig. 4).

272 These continuous annual series have been compared with temperature (daily maximum, minimum and
273 mean), precipitation, potential evaporation, and glacier melt of the pre-monsoon, monsoon (Fig. 5), and
274 post-monsoon seasons. All these trends are noted in Figure SI4, and a correlation table comparing pond
275 surface area variations and potential drivers of change is presented in Table SI5. In general, we observe
276 from this table that the highest correlations are found for the monsoon period. The reason is because 90%
277 of the precipitation and the highest temperatures are recorded during this period (Salerno et al., 2015).
278 Consequently, the main hydrological processes in the Himalaya occur during the monsoon season.
279 Focusing on this season, we first observe a large and significant precipitation decrease (-11 mm yr^{-1} ;
280 $p < 0.1$) (Fig. 6a; Fig. SI4). Even the mean temperature decreases, but slightly and not significantly (Fig.
281 SI4). This is a result of a significant decrease in maximum temperature ($-0.08 \text{ }^{\circ}\text{C yr}^{-1}$; $p < 0.05$) (Fig. 6b;
282 Fig. SI4) balanced by an increase in minimum temperature (Fig. SI4). The potential evaporation,
283 calculated on the basis of the mean temperature and global radiation, is constant during the summer
284 period. These trends have been more broadly discussed in Salerno et al., 2015. These authors, for a longer
285 period (since 1994), observed that the mean air temperature has increased by $0.9 \text{ }^{\circ}\text{C}$ ($p < 0.05$) at the
286 annual level but that warming has occurred mainly outside the monsoon period and mainly in the
287 minimum temperatures. Moreover, as we observed here for the last decade, a decrease in maximum
288 temperature from June to August ($-0.05 \text{ }^{\circ}\text{C yr}^{-1}$, $p < 0.1$) has been observed. In terms of precipitation, a
289 substantial reduction during the monsoon season (47%, $p < 0.05$) has been observed.



290 The glacier melt related to each glacier within the pond basins has been calculated considering both
291 the both maximum and mean daily temperatures. The averages for all selected cases are analyzed for each
292 season in Figure SI4, which reveals that the only period producing a sensible contribution is the monsoon
293 period if the maximum daily temperatures are considered the main driver of the process. The reason can
294 be easily observed in Figure 2b, which shows the 0 °C isotherms corresponding to the mean and
295 maximum temperatures. Only the 0 °C isotherm related to the daily maximum temperature during the
296 monsoon period is located higher than mean elevation of the analyzed glaciers. The T-index model only
297 calculates the melting associated with temperatures above 0 °C, thereby explaining this pattern. In other
298 words, the diurnal temperatures influence the melting processes much more the nocturnal ones, which are
299 considered in the mean daily temperature. Figure 6b shows that the trend is significantly decreasing (3%
300 yr⁻¹, p<0.05), according to the decrease observed in maximum temperature.

301 As anticipated, the highest correlations between ponds surface areas and potential drivers are found
302 for the monsoon period. Based on Table SI5, we observe that precipitation, maximum monsoon
303 temperature, and relevant glacier melt are the main drivers of change. The PCA shown in Figure 5
304 attempts to provide an overall overview of the relationships, during the monsoon period, among the trends
305 related to the potential drivers of change and the pond surface areas. This representation helps to further
306 summarize the main components of the water balance system that influence the pond surface areas, i.e.,
307 glacier melt and precipitation. We observe that evaporation is not a sensible factor at these elevation and
308 that the evaporation/precipitation ratio is approximately 0.41. Therefore, a hypothetical variation in the
309 precipitation regime affects the pond water balance two and half times more than the same variation in the
310 evaporation rate. Moreover, from Figure 5, we observe that there are some ponds that are more correlated
311 with the monsoon precipitation (i.e., LCN76, LCN141, LCN77, LCN11, and LCN93) and others that are
312 more correlated with the glacier melt (i.e., LCN68, LCN3, and LCN9). A few ponds seem influenced by
313 both drivers (i.e., LCN24 and LCN139). The coefficients of correlation are reported in Table 4. According
314 to the grouping observed with the PCA, Figure 6 shows good fits between the pond surface area trends
315 and the main drivers of change. Based on Table 4, ponds with higher glacier coverage within the basis
316 show higher correlations with the glacier melt, and, in contrast, ponds with lower glacier coverage show
317 higher correlations with precipitation. In our case study, the threshold between the two groups appears to
318 be a glacier coverage of 10%.

319 **4.4 Analysis of ponds surface area in the last fifty years.**

320 Based on the findings related to the main drivers of changes that have influenced the 10 selected
321 ponds, the overall pond population (all 64 ponds) has been subdivided into two classes defined in relation
322 to the glacier cover (%) in their basins. In 2013, 25 ponds presented a glacier cover > 10% (i.e., 40% of
323 the total ponds), and 39 ponds (i.e., 60% of the total ponds) featured glacier coverages less than this
324 threshold. Hereafter, we define these ponds as ponds without glaciers in the basin (ponds-without-
325 glaciers), neglecting in this way relatively small glacier bodies, which could possibly be confused with
326 snowfields. The opposite class is defined as ponds with glaciers in the basin (ponds-with-glaciers).
327 Among ponds-with-glaciers, Table 2 shows that they are characterized by a median glacier coverage of
328 19%, oriented toward the east-southeast and very steep (31°).

329 The observed changes according to this new classification are reported in Table 3. The maps in Figure
330 7 show the spatial differences between the two classes and comparing the relative annual rate of change,
331 whereas Figure 8 traces their trends over time. We have already discussed (Fig. 4) that, in general, all
332 unconnected ponds over the last fifty years have decreased by approximately 10%. Additionally, the



333 presence of glaciers within the pond basins results in divergent trends. The surface area of ponds-without-
334 glaciers, from 1963 to 2013, strongly decreased ($-25\pm6\%$, $p<0.001$), whereas, for the same period, the
335 surface area of ponds-with-glaciers decreased much less ($-6\pm2\%$, $p<0.05$). Differences in behavior are
336 also noticeable during the intermediate periods. In this case, we compare the median values of the relative
337 annual rates of change. From 1963 to 1992, ponds-without-glaciers increased slightly ($0.9\pm0.5\% \text{ yr}^{-1}$,
338 $p<0.1$), whereas the other ones remained constant ($0.0\pm0.1\% \text{ yr}^{-1}$). From 1992 to 2000, ponds-without-
339 glaciers decreased slightly ($-1.1\pm1.9\% \text{ yr}^{-1}$, $p>0.1$), whereas the other ones increased slightly but
340 significantly ($+0.7\pm0.5\% \text{ yr}^{-1}$, $p<0.05$). In the most recent period (2000 to 2013), both categories
341 decreased, but ponds-without-glaciers decreased more ($-2.3\pm0.7\% \text{ yr}^{-1}$, $p<0.001$; $-1.5\pm0.4\% \text{ yr}^{-1}$,
342 $p<0.001$).

343 The significance of the divergent trend observed between the two groups has been tested for two
344 periods (1963-1992 and 1992-2013). Ponds-without-glaciers featured significantly ($p<0.01$) higher
345 increases than ponds-with-glaciers in the first period ($+13\pm12\%$; $0\pm3\%$, respectively) and significantly
346 ($p<0.01$) higher decreases in the second period ($-38\pm6\%$; $-6\pm2\%$, respectively), based on a Kruskal-Wallis
347 test.

348

349 **4.5 Change in ponds surface area versus morphological boundary conditions.**

350 We also analyzed whether ponds belonging to the two classes experienced changes in surface area in
351 relation to certain morphological boundary conditions, such as the aspect or elevation of the basin. In this
352 case, we apply the Kruskal-Wallis test as the relevant post-hoc test described above. Figure 9 shows the
353 surface area changes observed during the 1992-2013 period. The changes were independent of both
354 elevation and aspect for ponds-without-glaciers (Fig. 9a; Fig. 9c), whereas significant differences can be
355 observed for ponds-with-glaciers. Ponds located at higher elevations experienced greater decreases (Fig.
356 9b). In particular, ponds over 5400 m a.s.l. decreased significantly ($p<0.01$) more than ponds located
357 below 5100 m a.s.l. In terms of aspect, the south-oriented ponds (Fig. 9d) experienced greater decreases,
358 which was significantly different from southeast ($p<0.01$) and southwest ($p<0.01$) orientations.

359 The tracing of pond surface areas provides furthermore information on precipitation and glacier melt
360 trends in space. The decline of precipitation in the SNP since 1992 occurred homogeneously at all
361 elevations and in all valleys independent of their orientation. Based on the greater loss of surface area for
362 ponds-with-glaciers at lower elevations, we can infer that glacier melt is higher at these elevations, surely
363 due to the effect of higher temperatures. Even in valleys oriented in directions other than south, we
364 observe greater losses in surface area for ponds-with-glaciers. Small glaciers lying in perpendicular
365 valleys, which are much steeper than the north-south-oriented valleys (following the monsoon direction),
366 are likely melting more due to their small size and higher gravitational stresses (e.g., Bolch et al., 2008;
367 Quincey et al., 2009).

368 **Conclusion**

369 In high-elevation Himalayan areas, glacial ponds have demonstrated a high sensitivity to climate
370 change. In general, over the last fifty years, unconnected ponds have decreased significantly by
371 approximately 10%. We attribute this change to both a drop in precipitation and a decrease in glacier melt
372 caused by a decline in the maximum temperature in the recent years. The continued shrinkage of glaciers
373 likely due to the effects of less precipitation than an increase in temperature. Evapotranspiration has little
374 effect at these elevations and has remained constant over the last decade, during which the main decline
375 in ponds surface area has been observed.



376 However, the main contribution provided by this study is to have demonstrated for our case study that
377 pond surface areas could be traced to detect the behavior of precipitation and glacier melt in remote and
378 barely accessible regions where, even for recent decades, few or no time series exist. Unfortunately,
379 before the 2000s, the availability of high-resolution satellite imagery is very limited. However, with the
380 limited data at our disposal, important information on the evolution of certain main components of the
381 hydrological cycle at high elevations has been discerned: an increase in precipitation occurred until the
382 middle 1990s followed by a decrease until recently. Until the 1990s, the glacier melt was constant. Then,
383 an increase occurred in the early 2000s. In recent years, the declining trend observed for maximum
384 temperature has reduced the glacier melt.

385 We observed that simply tracing the glacier surface areas did not yield information on the temporal
386 behavior of glacier melt. In this regard, a decrease in glacier surface area has been identified over the last
387 fifty years, but this reduction does not correspond to an increase in glacier melt, as normally expected. As
388 discussed by other authors (Thakuri et al., 2014; Salerno et al., 2015; Wagnon et al., 2013), on the south
389 slopes of Mt. Everest, the weaker precipitation is the main cause of glacier shrinkage. In recent years,
390 glaciers are accumulating less than they were decades ago; thus, their size is declining. In contrast, the
391 tracing of pond surface areas demonstrates that glacier melt has not increased during the same period. In
392 fact, the increase in mean air temperature here occurred mainly outside of the summer months and mainly
393 during the night (Salerno et al., 2015).

394 Consequently, a question arises in regard to the portability of this method. Here, portability refers to
395 the degree to which the proposed method is replicable in other remote environments. In the Himalaya,
396 other land based climatic series at high elevations are decidedly scarce (Barry, 2012; Rangwala and
397 Miller, 2012; Pepin et al., 2015; Salerno et al., 2015). This constraint limits the ability to further test the
398 ability of glacier ponds to detect the main water balance components in other Himalayan high-elevation
399 regions. Therefore, the inferences developed here could be simply applied and trends in precipitation and
400 glacier melt inferred for the overall mountain range. Observing differences in the magnitude of changes
401 between the two classes that differ in glacier coverage (threshold of 10%) across different periods, along
402 an elevation gradient, or according to the basin aspect, as carried out here, could improve the confidence
403 of the inferred findings. In contrast, in other mountain ranges with other the climatic conditions, the
404 inferences developed here might not be valid, and station-observed climatic data would be required to test
405 the ability of glacier ponds to detect the main water balance components.

406
407 **Author contributions**

408 F.S. and G.T. designed research; F.S. N.G. and S.T. analyzed data; F.S. wrote the paper. F.S. N.G. S.T.
409 G.V. and G.T. data quality check.

410 **Acknowledgements**

411 This work was supported by the MIUR through Ev-K2-CNR/SHARE and CNR-DTA/NEXTDATA
412 project within the framework of the Ev-K2-CNR and Nepal Academy of Science and Technology
413 (NAST).

414 **References**

415 Adrian, R., O'Reilly, C. M., Zagarese, H., Baines, S.B., Hessen, D.O., Keller, W., Livingstone, D. M.,
416 Sommaruga, R., Straile, D., van Donk, E., Weyhenmeyer, G. A., and Winderl, M.: Lakes as sentinels
417 of climate change, Limnol. Oceanogr., 54, 2283–2297, doi:10.4319/lo.2009.54.6_part_2.2283, 2009.
418 Ageta, Y. and Fujita, K.: Characteristics of mass balance of summeraccumulation type glaciers in the



419 Himalayas and Tibetan Plateau, Z. Gletscherkd, Glazialgeol., 32, 61–65, 1996
420 Ageta, Y., Iwata, S., Yabuki, H., Naito, N., Sakai, A., Narama, C., and Karma, T.: Expansion of glacier
421 lakes in recent decades in the Bhutan Himalayas, IAHS Publication, 264, 165–175, 2000.
422 Amatya, L. K., Cuccillato, E., Haack, B., Shadie, P., Sattar, N., Bajracharya, B., Shrestha, B., Caroli, P.,
423 Panzeri, D., Basani, M., Schommer, B., Flury, B., Salerno, F., and Manfredi, E. C.: Improving
424 communication for management of social-ecological systems in high mountain areas: Development of
425 methodologies and tools – The HKKH Partnership Project, Mt. Res. Dev., 30, 69–79,
426 doi:10.1659/MRD-JOURNAL-D-09-00084.1, 2010.
427 Bajracharya B., Uddin, K., Chettri, N., Shrestha, B., and Siddiqui, S. A.: Understanding land cover
428 change using a harmonized classification system in the Himalayas: A case study from Sagarmatha
429 National Park, Nepal, Mt. Res. Dev., 30, 143–156, doi: 10.1659/MRD-JOURNAL-D-09-00044.1,
430 2010.
431 Barry, R. G.: Recent advances in mountain climate research, Theor. Appl. Climatol., 110, 549–553,
432 doi:10.1007/s00704-012-0695-x, 2012.
433 Beniston, M.: Mountain weather and climate: A general overview and a focus on climatic change in the
434 Alps, Hydrobiologia, 562, 3–16, doi: 10.1007/s10750-005-1802-0, 2006.
435 Benn, D. I., Bolch, T., Hands, K., Gulley, J., Luckman, A., Nicholson, L. I., Quincey, D., Thompson, S.,
436 Toumi, R., Wiseman, and S.: Response of debris-covered glaciers in the Mount Everest region to re-
437 cent warming, and implications for outburst flood hazards. Earth-Sci. Rev., 114, 156–174,
438 doi:10.1016/j.earscirev.2012.03.008, 2012.
439 Benn, D., Wiseman, S., and Hands, K.: Growth and drainage of supraglacial lakes on debris mantled
440 Ngozumpa Glacier, Khumbu Himal, Nepal, J. Glaciol., 47 (159), 626–638,
441 doi:<http://dx.doi.org/10.3189/172756501781831729>, 2001.
442 Bhuju, D. R., Carrer, M., Gaire, N. P., Soraruf, L., Riondato, R., Salerno, F., and Maharjan, S. R.: Den-
443 droecological study of high altitude forest at Sagarmatha National Park, Nepal, in: Contemporary Re-
444 search in Sagarmatha (Mt. Everest) Region, Nepal: An Anthology, edited by: Jha, P. K. and Khanal, I.
445 P., Nepal Academy of Science and Technology, Kathmandu, Nepal, 119–130, 2010.
446 Bolch, T., Buchroithner, M., Pieczonka, T., and Kunert, A.: Planimetric and volumetric glacier changes in
447 the Khumbu Himal, Nepal, since 1962 using Corona, Landsat TM and ASTER data, J. Glaciol., 54,
448 592–600, doi: 10.3189/002214308786570782, 2008.
449 Bolch, T., Kulkarni, A., Kääb, A., Huggel, C., Paul, F., Cogley, J. G., Frey, H., Kargel, J. S., Fujita, K.,
450 Scheel, M., Bajracharya, S., and Stoffel, M.: The state and fate of Himalayan glaciers, Science, 336,
451 310–314, 2012.
452 Bolch, T., Pieczonka, T., and Benn, D. I.: Multi-decadal mass loss of glaciers in the Everest area (Nepal
453 Himalaya) derived from stereo imagery, The Cryosphere, 5, 349–358, doi:10.5194/tc-5- 349-2011,
454 2011.
455 Buraschi, E., Salerno, F., Monguzzi, C., Barbiero, G., and Tartari, G.: Characterization of the Italian lake-
456 types and identification of their reference sites using anthropogenic pressure factors, J. Limnol. 64,
457 75–84, doi: <http://dx.doi.org/10.4081/jlimnol.2005.75>, 2005.
458 Fox, J. and Weisberg, S.: An R Companion to Applied Regression, Second Edition, Sage, 2011.
459 Frey, H., Paul, F., and Strozzi, T.: Compilation of a glacier inventory for the western Himalayas from
460 satellite data: methods, challenges and results, Remote Sens. Environ., 124, 832–843, 2012
461 Fujita, K., Sakai, A., Nuimura, T., Yamaguchi, S., and Sharma, R.: Recent changes in Imja Glacial lake
462 and its damming moraine in the Nepal Himalaya revealed by in situ surveys and multi-temporal
463 ASTER imagery, Environ. Res. Lett., 4, 1–7, doi: <http://dx.doi.org/10.1088/1748-9326/4/4/045205>,
464 2009.
465 Gardelle, J., Arnaud, Y., and Berthier, E.: Contrasted evolution of glacial lakes along the Hindu Kush
466 Himalaya mountain range between 1990 and 2009, Global Planet. Change, 75, 47–55, 2011.
467 Gulley, J., and Benn D.: Structural control of englacial drainage systems in Himalayan debris-covered
468 glaciers, J. Glaciol., 53, 399–412, doi:10.3189/002214307783258378, 2007.



469 Guyennon, N., Romano, E., Portoghesi, I., Salerno, F., Calmant, S., Petraneli, A. B., Tartari, G., and
470 Copetti, D.: Benefits from using combined dynamical-statistical downscaling approaches – lessons
471 from a case study in the Mediterranean region, *Hydrol. Earth Syst. Sc.*, 17, 705–720,
472 doi:10.5194/hess-17-705-2013, 2013.

473 Hamerlik, L., Svitok, M., Novíkmeč, M., Ocadlík, M., and Bitusík, P.: Local among-site and regional
474 diversity patterns of benthic macroinvertebrates in high altitude waterbodies: do ponds differ from
475 lakes?, *Hydrobiologia*, doi: 10.1007/s10750-013-1621-7, 2013.

476 Hervé, M.: Diverse Basic Statistical and Graphical Functions (RVAideMemoire). R package, 2015.

477 Hock, R.: Temperature index melt modeling in mountain areas, *J. Hydrol.*, , 282, 104–115, doi:
478 10.1016/S0022-1694(03)00257-9, 2003.

479 Hothorn, T., Hornik K., van de Wiel, M. A., Wiel, H., and Zeileis, A.: Conditional Inference Procedures,
480 R package, 2015.

481 Ichiyanagi, K., Yamanaka, M. D., Muraji, Y., and Vaidya, B. K.: Precipitation in Nepal between 1987
482 and 1996, *Int. J. Climatol.*, 27, 1753–1762, doi:10.1002/joc.1492, 2007.

483 Jensen, M. E., and Haise, H. R.: Estimating evapotranspiration from solar radiation, *J. Irrig. Drain. Div.*,
484 Am. Soc. Civ. Eng., , 89, 15–41, 1963.

485 Kääb, A., Berthier, E., Nuth, C., Gardelle, J., and Arnaud, Y.: Contrasting patterns of early twenty-first-
486 century glacier mass change in the Himalayas, *Nature*, 488, 495–498, doi:10.1038/nclimate1580,
487 2012.

488 Kayastha, R. B. and Harrison, S. P.: Changes of the equilibriumline altitude since the little ice age in the
489 Nepalese Himalaya, *Ann. Glaciol.*, 48, 93–99, 2008.

490 Kendall, M. G.: *Rank Correlation Methods*, Oxford University Press, New York, 1975.

491 Lami, A., Marchetto, A., Musazzi, S., Salerno, F., Tartari, G., Guilizzoni, P., Rogora, M., Tartari, G. A.:
492 Chemical and biological response of two small lakes in the Khumbu Valley, Himalayas (Nepal) to
493 short-term variability and climatic change as detected by long term monitoring and paleolimnological
494 methods, *Hydrobiologia*, 648, 189–205, doi: 10.1007/s10750-010-0262-3, 2010.

495 Lei, Y., Yang, K., Wang, B., Sheng, Y., Bird, B. W., Zhang, G., and Tian, L.: Response of inland lake
496 dynamics over the Tibetan Plateau to climate change, *Clim. Change*, 125, 281–290
497 doi:10.1007/s10584-014-1175-3, 2014.

498 Liu, Q., Mayer, C., and Liu S.: Distribution and interannual variability of supraglacial lakes on debris-
499 covered glaciers in the Khan Tengri-Tomur Mountains, Central Asia, *Environ. Res. Lett.*, 10, 4545-
500 4584, doi:10.5194/tcd-7-4545-2013, 2015.

501 Loibl, D. M. , Lehmkühl, F. , and Grießinger, J.: Reconstructing glacier retreat since the Little Ice Age in
502 SE Tibet by glacier mapping and equilibrium line altitude calculation, *Geomorphology*, 214, 22–
503 39,doi: 10.1016/j.geomorph.2014.03.018, 2014.

504 Mann, H. B.: Nonparametric tests against trend, *Econometrica*, 13, 245–259, 1945.

505 Pepin N., Bradley R. S., Diaz H. F., Baraer M., Caceres E. B., Forsythe N., Fowler H., Greenword G.,
506 Hashmi M. Z., Liu X. D., Miller J. D., Ning L., Ohmura A., Palazzi E., Rangwala I., Schoner W.,
507 Severskiy I., Shahgedanova M., Wang M. B., Williamson S. N., and Yang D. Q.: Elevation-
508 dependent warming in mountain regions of the world. *Nature Clim. Change*, 5(5), 424–430, doi:
509 10.1038/nclimate2563, 2015.

510 Pham, S. V., Leavitt, P. R., McGowan, S., Peres-Nato, P.: Spatial variability of climate and land-use ef-
511 fects on lakes of the northern Great Plains, *Limnol. Oceanogr.* 53, 728–742, doi:
512 10.4319/lo.2008.53.2.0728, 2008.

513 Pohlert, T.: The Pairwise Multiple Comparison of Mean Ranks Package (PMCMR), R package. 2014.

514 Quincey, D. J., Luckman, A., and Benn, D.: Quantification of Everest region glacier velocities between
515 1992 and 2002, using satellite radar interferometry and feature tracking, *J. Glaciol.*, 55, 596–606, doi:
516 http://dx.doi.org/10.3189/002214309789470987, 2009.



517 Quincey, D., Richardson, S., Luckman, A., Lucas, R., Reynolds, J., Hambrey, M., and Glasser, N.: Early
518 recognition of glacial lake hazards in the Himalaya using remote sensing datasets, *Global Plan.*
519 *Change*, 56, 137-152, doi:10.1016/j.gloplacha.2006.07.013, 2007.

520 Rangwala, I., and Miller, J. R.: Climate change in mountains: a review of elevation-dependent warming
521 and its possible causes, *Clim. Change*, 114, 527-547, doi: 10.1007/s10584-012-0419-3, 2012.

522 Reynolds, J.: On the formation of supraglacial lakes on debris-covered glaciers, IAHS publication, 264,
523 153-161, doi: 10.3189/002214310791190785, 2000.

524 Richardson, S. D., and Reynolds J. M.: An overview of glacial hazards in the Himalayas, *Quatern. Int.*,
525 65-66, 31-47, doi:10.1016/S1040-6182(99)00035-X, 2000.

526 Sakai, A., and Fujita K.: Formation conditions of supraglacial lakes on debris covered glaciers in the
527 Himalaya, *J. Glaciol.*, 56, 177-181, doi: 10.3189/002214310791190785, 2010.

528 Sakai, A.: Glacial lakes in the Himalayas: A review on formation and expansion processes, *Glob. Environ.*
529 *Res.*, 16, 23-30, 2012.

530 Salerno, F., Cuccillato, E., Caroli, P., Bajracharya, B., Manfredi, E. C., Viviano, G., Thakuri, S., Flury, B.,
531 Basani, M., Giannino, F., and Panzeri, D.: Experience with a hard and soft participatory modeling
532 framework for social ecological system management in Mount Everest (Nepal) and K2 (Pakistan)
533 protected areas, *Mt. Res. Dev.*, 30, 80-93, doi: <http://dx.doi.org/10.1659/MRD-JOURNAL-D-10-00014.1>, 2010.

535 Salerno, F., Gambelli, S., Viviano, G., Thakuri, S., Guyennon, N., D'Agata, C., Diolaiuti, G., Smiraglia,
536 C., Stefani, F., Bochhiola, D., and Tartari, G.: High alpine ponds shift upwards as average temperature
537 increase: A case study of the Ortles-Cevedale mountain group (Southern alps, Italy) over the last 50
538 years, *Global Planet. Change*, doi: 10.1016/j.gloplacha.2014.06.003, 2014a.

539 Salerno, F., Guyennon, N., Thakuri, S., Viviano, G., Romano, E., Vuillermoz, E., Cristofanelli, P., Stoc-
540 chi, P., Agrillo, G., Ma, Y., and Tartari, G.: Weak precipitation, warm winters and springs impact
541 glaciers of south slopes of Mt. Everest (central Himalaya) in the last 2 decades (1994–2013), *Cry-
542 osphere*, 9, 1229-1247, doi:10.5194/tc-9-1229-2015, 2015.

543 Salerno, F., Thakuri, S., D'Agata, C., Smiraglia, C., Manfredi, E. C., Viviano, G., and Tartari, G.: Glacial
544 lake distribution in the Mount Everest region: Uncertainty of measurement and conditions of for-
545 mation, *Global Planet. Change*, 92-93, 30-39, doi:10.1016/j.gloplacha.2012.04.001, 2012.

546 Salerno, F., Viviano, G., Carraro, E., Manfredi, E. C., Lami, A., Musazzi, S., Marchetto, A., Guyennon,
547 N., Tartari, G., and Copetti, D.: Total phosphorus reference condition for subalpine lakes: comparison
548 among traditional methods and a new process based and dynamic lake-basin approach, *J. Environ.*
549 *Manag.*, 145, 94-105, doi:10.1016/j.jenvman.2014.06.011, 2014b.

550 Salerno, F., Viviano, G., Mangredi, E. C., Caroli, P., Thakuri, S., and Tartari, G.: Multiple Carrying Ca-
551 pacities from a management-oriented perspective to operationalize sustainable tourism in protected
552 area, *J. Environ. Manag.*, 128, 116-125, doi:10.1016/j.jenvman.2013.04.043, 2013.

553 Scherler, D., Bookhagen, B., and Strecker, M. R.: Spatially variable response of Himalayan glaciers to
554 climate change affected by debris cover, *Nat. Geosci.*, 4, 156–159, 2011.

555 Settle, S., Goonetilleke, A., and Ayoko, G. A.: Determination of Surrogate Indicators for Phosphorus and
556 Solids in Urban Storm water: Application of Multivariate Data Analysis Techniques, *Water Air Soil*
557 *Poll.*, 182, 149-161, doi: 10.1007/s11270-006-9328-2, 2007.

558 Shapiro, S. S., and Wilk, M. B.: An analysis of variance test for normality (complete samples),
559 *Biometrika*, 52, 591–611, 1965.

560 Smith, L. C., Sheng, Y., MacDonald, G. M., and Hinzman, L. D.: Disappearing Arctic Lakes, *Science*,
561 308, 1429-1429, doi: 10.1126/science.1108142, 2005.

562 Smol, J. and Douglas, M.: From controversy to consensus: Making the case for recent climate change in
563 the Arctic using lake sediments, *Front. Ecol. Environ.*, 5, 466-474, doi: 10.1890/060162, 2007.

564 Somos-Valenzuela, M. A., McKinney, D. C., Rounce, D. R., and Byers, A. C.: Changes in Imja Tsho in
565 the Mount Everest region of Nepal, *Cryosphere* 8, 1661–1671., doi: 10.5194/tc-8-1661-2014, 2014.

566 Song, C., Huang, B., and Ke, L.: Heterogeneous change patterns of water level for inland lakes in High



567 Mountain Asia derived from multi-mission satellite altimetry, *Hydrol. Process.*, 29, 2769–2781, doi:
568 10.1002/hyp.103992015, 2015.

569 Tartari, G. Previtali, L, and Tartari, G. A.: Genesis of the lake cadastre of Khumbu Himal Region
570 (Sagarmatha National Park, East Nepal), in: Limnology of high altitude lakes in the Mt Everest Re-
571 gion (Nepal), edited by: Lami, A., and Giussani, G., *Mem. Ist. ital. Idrobiol.*, 57, 139-149, 1998.

572 Tartari, G., Salerno, F., Buraschi, E., Brucolieri, G., and Smiraglia, C.: Lake surface area variations in the
573 North-Eastern sector of Sagarmatha National Park (Nepal) at the end of the 20th Century by compari-
574 son of historical maps, *J. Limnol.*, 67, 139-154, doi:10.4081/jlimnol.2008.139, 2008.

575 Thakuri, S., Salerno, F., Bolch, T., Guyennon, N., and Tartari, G.: Factors controlling the accelerated
576 expansion of Imja Lake, Mount Everest region, Nepal, *Ann. Glaciol.*, 57, 245–257,
577 doi:10.3189/2016AoG71A063, 2015.

578 Thakuri, S., Salerno, F., Smiraglia, C., Bolch, T., D'Agata, C., Viviano, G., and Tartari, G.: Tracing
579 glacier changes since the 1960s on the south slope of Mt. Everest (central southern Himalaya) using
580 optical satellite imagery, *The Cryosphere*, 8, 1297-1315, doi:10.5194/tc-8-1297-2014, 2014.

581 Thompson, L. G., Thompson, E. M., Brecher, H., Davis, M., Leon, B., Les, D., Lin, P. N., Mashootta, T.,
582 and Mountain, K.: Abrupt tropical climate change: Past and present, *Proc. Natl. Acad. Sci. USA*, 103,
583 10536–10543, 2006.

584 Venables, W. N., and Ripley, B. D.: *Modern Applied Statistics with S*, Springer, New York, 2002.
585 carr

586 Vuille, M.: Climate variability and high altitude temperature and precipitation, in: *Encyclopedia of snow,*
587 ice and glaciers, edited by: Singh, V. P., Singh, P., and Haritashya, U. K., Springer, 153– 156, 2011.

588 Wagnon, P., Vincent, C., Arnaud, Y., Berthier, E., Vuillermoz, E., Gruber, S., Ménégoz, M., Gilbert, A.,
589 Dumont, M., Shea, J. M., Stumm, D., and Pokhrel, B. K.: Seasonal and annual mass balances of Mera
590 and Pokalde glaciers (Nepal Himalaya) since 2007, *The Cryosphere*, 7, 1769–1786, doi:10.5194/tc-7-
591 1769- 2013, 2013.

592 Wang, W., Xiang, Y., Gao, Y., Lu, A., and Yao, T.: Rapid expansion of glacial lakes caused by climate and
593 glacier retreat in the Central Himalayas, *Hydrol. Process.*, 29, 859–874, doi:10.1002/hyp.10199, 2015.

594 Williamson, C. E., Dodds, W., Kratz, T. K., and Palmer, M.: Lakes and streams as sentinels of
595 environmental change in terrestrial and atmospheric processes, *Front. Ecol. Environ.* 6, 247–254, doi:
596 10.1890/070140, 2008.

597 Wold, S., Esbensen, K., and Geladi, P.: Principal component analysis. *Chemom. Intell. Lab.* 2, 37-52.
598 1987.

599 Xie A., Ren, J., Qin, X., and Kang S.: Reliability of NCEP/NCAR reanalysis data in the
600 Himalayas/Tibetan Plateau, *J. Geographical Sciences*, doi: 10.1007/s11442-007-0421-2, 2007.

601 Yao, T., Thompson, L., Yang, W., Yu, W., Gao, Y., Guo, X., Yang, X., Duan, K., Zhao, H., Xu, B., Pu J.,
602 Lu A., Xiang Y., Kattel D. B., and Joswiak D.: Different glacier status with atmospheric circulations in
603 Tibetan Plateau and surroundings, *Nat. Clim. Change*, 2, 663-667, doi: 10.1038/nclimate1580, 2012.

604 Zhang, G., Yao, T., Xie, H., Wang, W., and Yang, W.: An inventory of glacial lakes in the Third Pole
605 region and their changes in response to global warming, *Glob. Planet. Change*, 131, 148–157,
606 doi:10.1016/j.gloplacha.2015.05.013, 2015.

607

608

609

610

611



612 **Table 1.** Coefficients of correlation between precipitation and temperature time series recorded at
 613 Pyramid station for the 1994-2013 period and gridded and reanalysis datasets (pre-monsoon, monsoon,
 614 and post-monsoon seasons as the months of February to May, June to September, and October to January,
 615 respectively). Bold values are significant with $p < 0.01$.

		APHRODITE	GPCC	CRU	ERA Interim
Precipitation	annual	0.43	0.75	0.34	0.33
Minimum Temperature	pre monsoon	0.64		0.81	
	monsoon	0.47		0.72	
	post monsoon	0.70		0.65	
	annual	0.72		0.92	
Mean Temperature	pre monsoon	0.79	0.83	0.8	0.87
	monsoon	0.61	0.51	0.42	0.67
	post monsoon	0.79	0.77	0.57	0.82
	annual	0.81	0.85	0.89	0.92
Maximum Temperature	pre monsoon	0.83			0.88
	monsoon	0.54			0.45
	post monsoon	0.82			0.86
	annual	0.70			0.80

616

617

618

619

620

621

622

623

624

625

626

627

628



629 **Table 2.** General summary of the morphological features of all the considered ponds (data from 2013).
 630

Topography	Glacier cover <5% median (range)	Glacier cover >5% median (range)	All lakes Median median (range)
Pond elevation (m a.s.l.)	5181(4460-5484)	5159(4505-5477)	5170(4460-5484)
Pond area (10^4 m 2)	0.8(0.1-6.2)	1.3(0.3-56.3)	1.1(0.1-56.2)
Basin area (10^4 m 2)	30(2-430)	130(30-2300)	70(2-2300)
Basin slope (°)	25(10-39)	29(23-41)	27(10-41)
Basin aspect (°)	163(68-256)	141(94-280)	159(68-280)
Basin mean elevation (m a.s.l.)	5293(4760-5531)	5400(5119-5945)	5315(4760-5945)
Basin/Lake area ratio (m 2 /m 2)	60(3-485)	67(10-523)	64(3-523)
Glacier area (%)	0(0-4)	19(0-61)	0.5(0-61)
Glacier slope (°)	-	31(21-38)	-
Glacier aspect (°)	-	124(150-250)	-
Glacier mean elevation (m a.s.l.)	-	5680(5470-7500)	-

631

632

633

634

635

636

637

638

639

640

641

642

643

644

645

646



647 **Table 3.** General summary of pond surface area changes from 1963 to 2013. The surface area changes of
 648 the glaciers located within the basins are also reported.

Period	Pond surface area change		Glacier surface area change		Period	Pond surface area change			
	Cumulative loss (%)		Cumulative loss (%)			Relative annual rate ($\% \text{ yr}^{-1}$)			
	Glacier coverage	< 5%	> 5%	All ponds	All basins	Glacier coverage	< 5%	> 5%	All ponds
1963-1992	+13 ± 12	0 ± 3	+3 ± 7	8 ± 8	1963-1992	0.9 ± 0.5	0.0 ± 0.1	+0.5 ± 0.3	
1963-2000	-1 ± 6	+9 ± 2 *	+7 ± 4	-2 ± 8	1992-2000	-1.1 ± 1.9	+0.7 ± 0.5 *	-0.4 ± 0.1	
1963-2008	-4 ± 5	+3 ± 2	+1 ± 4	-13 ± 9 **	2000-2008	-0.3 ± 1.0	-1.6 ± 0.6	-0.7 ± 0.7	
1963-2011	-7 ± 6	0 ± 2	-2 ± 5	-14 ± 14 **	2008-2011	0.0 ± 2.8	0.0 ± 1.6	0.0 ± 2.2	
1963-2013	-25 ± 6 ***	-6 ± 2 *	-10 ± 5 **	-26 ± 20 **	2011-2013	-12.9 ± 4.4 ***	-5.8 ± 2.5 *	-11 ± 3.5 **	
1992-2013	-38 ± 6 ***	-6 ± 2 *	-13 ± 5 **	-34 ± 15 ***	2000-2013	-2.3 ± 0.7 ***	-1.5 ± 0.4 ***	-1.7 ± 0.6 ***	

650

651

652

653

654

655

656

657

658

659

660

661

662

663

664

665

666

667



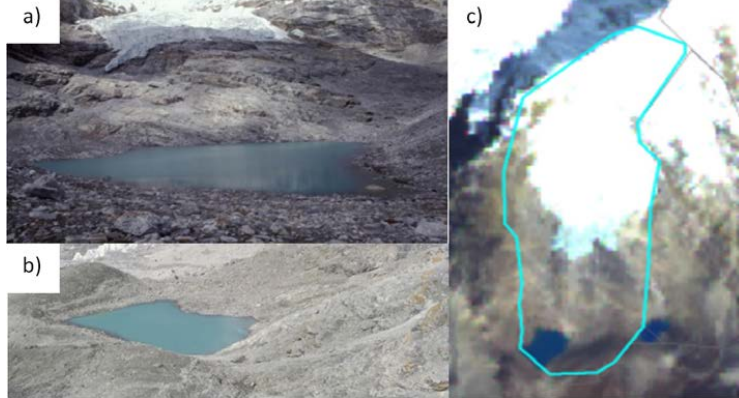
668 **Table 4.** Morphometric features of 10 selected ponds considered in the 2000-2013 analysis. Data are from
 669 2013. Coefficients of correlation are for the monsoon season. The relationships with the other seasons are
 670 reported in Table S15.

Pond Code	Glacier Cover (%)	Pond Elevation (m a.s.l.)	Basin Aspect (°)	Basin Slope (°)	Basin Area (km ²)	Pond Area (10 ⁴ m ²)	Basin Elevation (m a.s.l.)	Coefficient of Correlation (Ponds surface area vs Precipitation)	Coefficient of Correlation (Ponds surface area vs Glacier melt)
LCN139	1	4749	75	30	0.6	4.6	5596	0.50	0.35
LCN93	2	5244	116	23	0.7	0.6	5502	0.70 **	0.39
LCN141	3	5316	152	27	1.4	2.6	5701	0.72 **	0.37
LCN11	3	5029	229	24	1.2	1.8	5372	0.76 **	0.49
LCN77	7	4920	142	26	8.6	18.3	5507	0.55 *	0.29
LCN76	9	4800	140	25	13.6	59.2	5457	0.65 **	0.23
LCN24	10	4466	162	28	23.0	54.0	5477	0.44	0.65 **
LCN9	13	5202	117	36	0.7	0.6	5792	-0.27	0.61 **
LCN3	30	5261	154	35	2.0	11.7	5981	0.17	0.87 ***
LCN68	32	5006	232	35	1.2	3.2	5686	0.12	0.65 **
Median	8	5018	147	28	1.3	3.9	5551		

671

672

673



681

682

683 **Figure 1.** Example of an unconnected glacial pond (LCN5) with a glacier within the basin. Pictures were
 684 taken in September 1992: a) view looking north showing the distance between the glacier and the pond
 685 surface; b) from east showing the frontal moraine. c) LCN5 basin tracked on ALOS 2008 imagery.

686

687

688

689

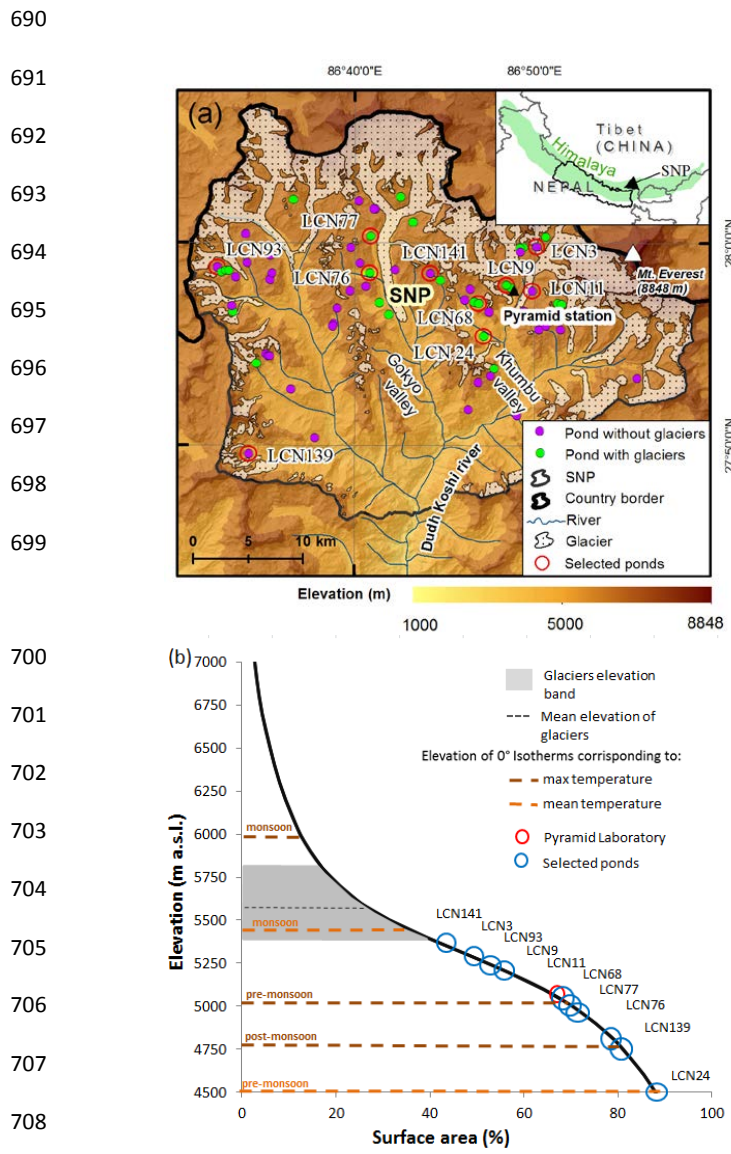
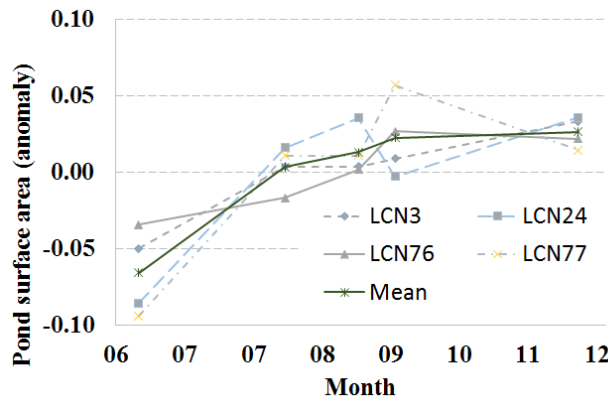


Figure 2. a) Location of the study area in the Himalaya and a detailed map of the spatial distribution of all unconnected ponds analyzed in this study. b) Hypsometric curve of SNP. Along this curve, the locations of 10 selected ponds are shown. The 0 °C isotherms corresponding to the mean and maximum temperature in 2013 are plotted for the pre-, post-, and monsoon period according to the lapse rates reported in Salerno et al., 2015. The mean glacier elevation distribution (mean \pm 1 standard deviation) of 10 selected ponds and the location of the...Pyramid meteorological station are also reported.



723 **Figure 3.** Intra-annual analysis (June-December) of selected pond surface areas

724

725

726

727

728

729

730

731

732

733

734

735

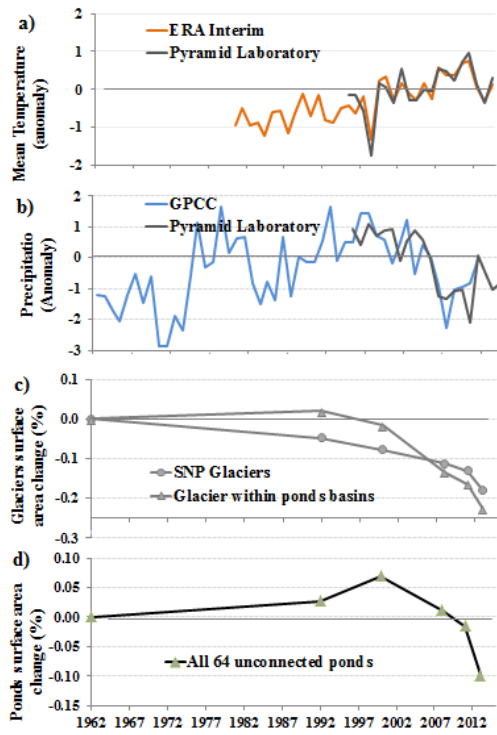
736

737

738

739

740



741

742 **Figure 4.** Trend analysis of climate, glacier area and ponds surface area for the last fifty years in the SNP.
743 a) and b) Trends are expressed in terms of anomalies with respect to the mean value calculated for the
744 considered period. c) and d) The relative variations with respect to 1963 are represented. a) Era Interim
745 mean annual temperature compared with Pyramid's land-based data. b) GPCC annual precipitation and
746 Pyramid's land-based data. c) Glacier surface area variations for the overall SNP (Thakuri et al., 2014)
747 and for glaciers located in basins with ponds. d) Surface area variations of the ponds.

748

749

750

751

752

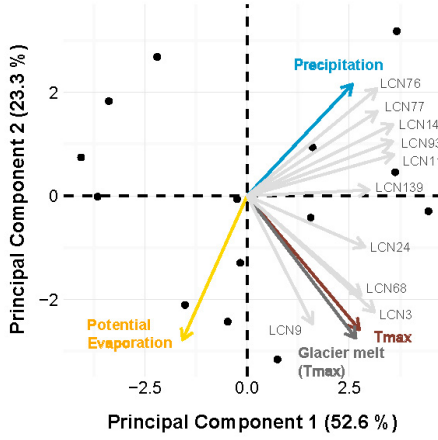
753

754

755



756



757

758 **Figure 5.** Principal Component Analyses (PCAs) between pond surface area from 2000 to 2013 and
759 potential drivers of change (maximum temperature, precipitation, glacier melt, and potential evaporation)
760 related to the monsoon season. Coefficients of correlation are reported in Table SI5. All trends related to
761 ponds and variables are provided in Figure SI1 and SI2.

762

763

764

765

766

767

768

769

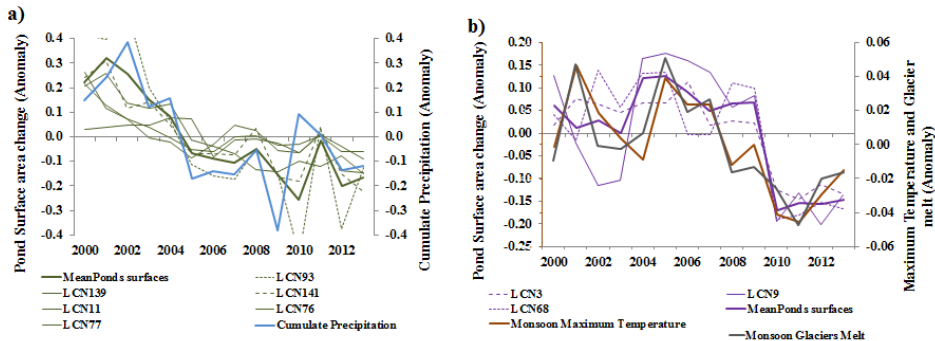
770

771

772

773

774



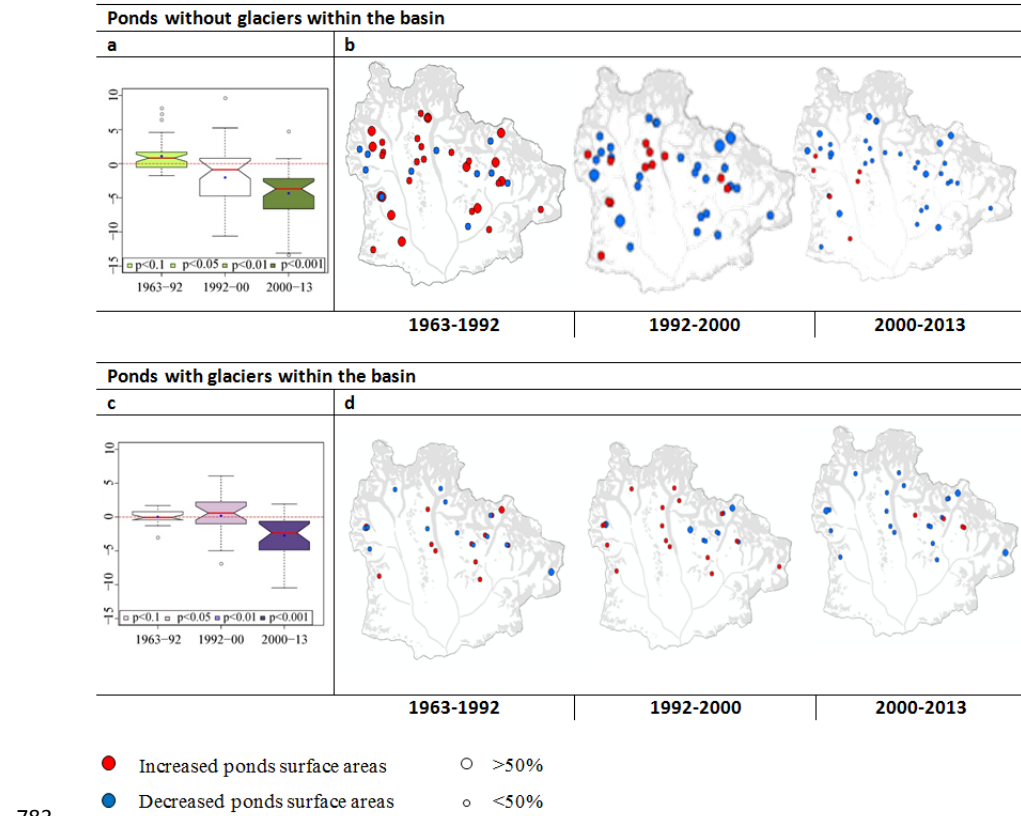
775

776 **Figure 6.** Annual trends from 2000 to 2013 related to pond surface area grouped according to the relevant
777 main drivers of change (monsoon season): a) glacier melt (maximum temperature), b) precipitation.
778 Coefficients of correlation are reported in Table SI5. All trends related to ponds and variables are
779 provided in Figure SI1 and SI2.

780

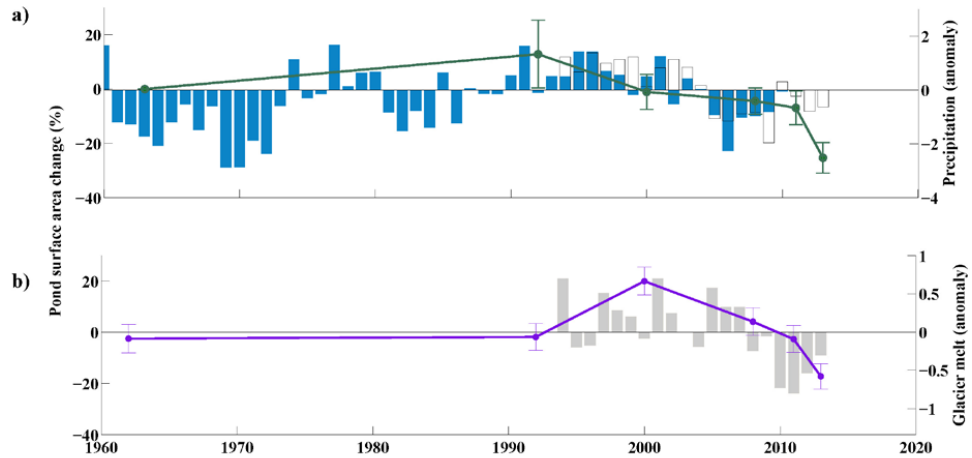
781

782



783

784 **Figure 7.** Changes in pond surface area in the Mt. Everest region. The left boxplots represent the annual
 785 rates of change of ponds in the analyzed periods: (a) ponds with glaciers within the basin, (c) ponds
 786 without glaciers within the basin. The blue points in the boxplots indicate the mean, whereas the red line
 787 is the median. On the right side, the maps (b, d) visualize the variations that occurred in the pond
 788 population during the same three periods considered in the relevant boxplots on the left. Reference data
 789 are reported in Table 3. All percentages refer to the initial year of the analysis (1963).



790

791 **Figure 8.** Trend analysis for the last fifty years of pond surface area in the SNP for a) ponds-without-
792 glaciers and b) ponds-with-glaciers.

793

794

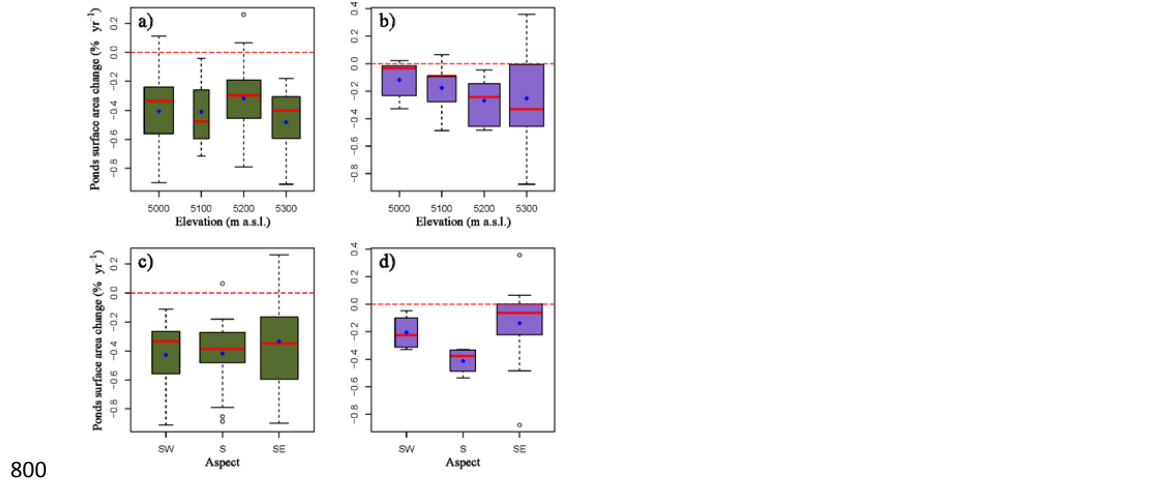
795

796

797

798

799



801 **Figure 9.** Pond surface area changes observed during the 1992–2013 period in relation to certain
802 morphological boundary conditions in the basin: elevation (upper graphs) and aspect (lower graphs). On
803 the left ponds-without-glaciers, and on the right ponds-with-glaciers.

804
805